

Monte Carlo calculations of nuclear cascades and associated Čerenkov radiation in extensive air showers

Jonathan E. Grindlay

Center for Astrophysics, Harvard College Observatory and Smithsonian Astrophysical Observatory, Cambridge, Massachusetts 02138

(Received 29 July 1974)

We present a Monte Carlo calculation, with observed cross sections and multiplicities, of the nuclear component of small extensive air showers (EAS) with primary energies $E_0 \geq 10^3$ GeV. The simulations were completely three-dimensional and were initiated by cosmic rays sampled from both their primary energy and mass spectra. Resulting particle spectra sampled at 564 g cm^{-2} agree with extrapolations from observations of EAS with $E_0 > 10^{4.6}$ GeV. The optical Čerenkov radiation calculated for the nuclear-active particles and muons in these EAS is found to be comparable to that expected from the electrons and distinguishable for particular detector configurations. Implications for EAS observations of cosmic γ rays and cosmic-ray composition are mentioned.

I. INTRODUCTION

With the attainment of laboratory energies of 300 and 1500 GeV in the Batavia and CERN (ISR) accelerators, the details of interactions at energies relevant to certain cosmic-ray studies have become available. While the extensive air showers (EAS) resulting from cosmic rays of primary energy $< 10^{14}$ eV contain too few particles to be directly detectable even at mountain altitudes, EAS from primary cosmic rays at energies > 100 GeV can be detected by the optical Čerenkov radiation they produce in the atmosphere. In fact, the cosmic-ray spectrum in the primary energy range $E_0 \sim 10^{11} - 10^{14}$ eV remains accessible only by this technique until long-exposure satellite detectors (such as HEAO-C) become available. Since the initial detection¹ of the atmospheric Čerenkov-radiation component of EAS, a number of experimental studies²⁻⁵ and theoretical calculations⁶⁻⁹ of the Čerenkov photon yield from EAS (electrons) have been conducted. However, none of these studies has explicitly considered the Čerenkov yield of the nuclear and meson cascade, and no simulations have been reported for those small (~ 1500 GeV) EAS for which the calculation can now be done "exactly" with known cross sections and multiplicities.

We began such a study¹⁰ in 1971 in an attempt to account for certain observed features⁵ of the Čerenkov angular distribution. This work led to a probable method of discriminating against normal cosmic-ray-initiated EAS in searches for EAS initiated by cosmic γ -ray sources. We shall now report the results of "exact" Monte Carlo simulations of the nuclear component of EAS vertically incident with $E_0 \geq 1000$ GeV and the resulting Čerenkov component. These calculations have employed the accelerator results for the p - p cross sections

and multiplicities, the measured fragmentation probabilities for the initial breakup of heavy cosmic-ray nuclei, the observed primary cosmic-ray energy spectrum, and several trial primary mass distributions. The results have been sampled for several particle-distribution functions that may be compared with those calculated and measurable for much larger EAS. Finally, the nuclear-component Čerenkov photon yield that would actually be detected by a system with a typical effective $A\Omega$ has been calculated. The relevance of these results is briefly considered for related efforts in ground-based γ -ray astronomy. A subsequent paper will compare some of these calculation results with particular experimental data to infer general features of the cosmic-ray composition at $E_0 > 10^{12}$ eV.

II. METHOD OF MONTE CARLO SIMULATION OF EAS

The cosmic-ray shower calculation was completely three-dimensional and was followed through 81 slabs of 9.4-g cm^{-2} -depth increment from the top of the atmosphere to 761.4 g cm^{-2} , the depth of many of our observations.¹⁰ At a given 9.4-g cm^{-2} slab, particles entering from above were considered in turn for their flight across the slab. If a given particle was found to interact or decay at a given depth, its interaction or decay products were individually followed out of the layer for possible interactions or decays in the succeeding slab. Thus, for every 9.4-g cm^{-2} atmospheric depth, a complete description of the nuclear-cascade particles was available and stored on magnetic tape. This description included the x and y position of each particle relative to the EAS axis and its delay relative to the shower "front," defined by a spherical wave propagating at c from the first interaction. Each particle's direction

cosines, energy, mass, and depth of origin were also stored, as well as the sum of all energy lost to the π_0 component down through the particular layer considered. Particles were no longer followed if they were found to decay into the electromagnetic component (e.g., muon-electron decays) or if they exceeded a cutoff radius (500 m) from the EAS axis. The accumulated energy loss into such particles was available at each layer.

Nuclear interactions were calculated for the initial breakup of the sampled primary nucleus in accordance with the appropriate fragmentation probabilities.^{11,12} In the breakup of very heavy primaries (e.g., iron), one or two nucleons were also sometimes allowed to undergo p - p interactions producing pions. Resulting individual nucleons (as well as, of course, primary nucleons) were tested at each layer d_i for possible interaction at depth d ,

$$d = d_i - \lambda(\ln R)\cos\theta_3, \quad (1)$$

where λ is the interaction-type mean free path, R is a computer-generated random number ($0 \leq R \leq 1.0$), and θ_3 is the particle zenith angle. If $d \leq d_{i+1}$, the interaction was calculated within the slab. The energy-dependent (above $E_{\text{lab}} = 1000$ GeV) p - p cross section given by Yodh *et al.*¹³ was used for the inelastic mean free path in air:

$$\begin{aligned} \lambda &= 90 \text{ g cm}^{-2} \quad (E < 1000 \text{ GeV}), \\ \lambda &= 90(39/\{38.8 + 0.4[\ln(2E/140)]^2\}) \text{ g cm}^{-2} \\ &\quad (E \geq 1000 \text{ GeV}). \end{aligned} \quad (2)$$

The mean free path for elastic scattering was taken as 4.5 times the inelastic value after the measurements at 300 GeV reported by Dao *et al.*¹⁴ The mean free path for pion inelastic collisions used was 120 g cm^{-2} . No energy dependence was assumed since almost all pions created had energies < 1000 GeV. The details of our interaction model for the production of pions and secondary nucleons were essentially the same as described previously,¹⁰ except that the expectation value for the multiplicity distribution of charged secondaries n_{ch} was now

$$\begin{aligned} \langle n_{\text{ch}}(n_{\text{ch}} - 1) \rangle &= 22.5 - 15.7 \ln E_{\text{c.m.}}^2 \\ &\quad + 3.83(\ln E_{\text{c.m.}}^2)^2, \end{aligned} \quad (3)$$

where $E_{\text{c.m.}}$ is the center-of-mass interaction energy, in accordance with a multiperipheral-model fit to accelerator data given by Berger.¹⁵ As before, a complete three-dimensional solution, with energy and momentum conservation, was obtained for each interaction. Only pions and nucleons were calculated as interaction products since the EAS development (for $E_0 < 10^{14}$ eV) is relatively

insensitive to kaon production and to the small numbers of antinucleons and other particles produced; that is, all interaction products other than the participating nucleons may be treated as pions. Also, since we were ultimately interested only in the nucleonic cascade particles that produce atmospheric Čerenkov radiation, particles with energy < 4.5 GeV (the Čerenkov threshold for muons) were no longer followed. Because of this relatively high minimum particle energy, ionization energy losses could be neglected, as well as the effects of multiple scattering and magnetic deflection on particle propagation in the atmosphere.

The energy E_0 of each primary cosmic ray initiating an EAS was sampled randomly from the known power-law spectrum $N(E)dE = KE_0^{-2.67}dE$ above a threshold of $E_0 = 1000$ GeV. The primary mass was sampled randomly from a trial cosmic-ray composition. Approximately 120 EAS were calculated first for the composition known¹⁶ for low-energy (< 10 GeV/nucleon) cosmic rays. An additional 275 EAS were calculated for a second trial composition in which the abundance of the very heavy primaries (predominantly iron nuclei) was increased by a factor of 3. As mentioned, the sensitivity of the EAS model to primary mass and detailed comparisons of these results with experimental data will be considered in a subsequent paper on cosmic-ray composition. Complete results for each EAS generated were stored on magnetic tape so that a complete description of the nuclear-cascade particles and total π_0 energies was available every 9.4-g cm^{-2} atmospheric depth. The calculations required about 3 hours of computer time on the Smithsonian CDC 6400.

The several tapes containing the calculated EAS could then be analyzed in a variety of ways. Our primary interest, however, was to calculate the atmospheric Čerenkov-radiation pattern produced by the individual particles in the calculated EAS. Thus, a program was written to read the EAS output tapes and calculate the Čerenkov production from each particle at the 9.4-g cm^{-2} -depth increments. The formulism summarized by Jelley¹⁷ was used to calculate, for each particle, the Čerenkov cone angle and the number of photons in the typically observed band (300–550 nm) per unit area incident on a detection plane at 761-g cm^{-2} atmospheric depth. The lateral photon density distribution was then calculated as a function of core radius and the photon angular distribution at any fixed core radius was also calculated. For comparison with measured photon angular distributions,^{5,10} the angular distributions detectable by $1\text{--}2^\circ$ (opening-angle) detectors were also calculated. Results could also be checked against variations in detected EAS arrival direction and core

radius by appropriate trial random variations in the generated EAS incidence angle and impact radius.

III. RESULTS OF THE CALCULATIONS

The EAS Monte Carlo simulations have been analyzed for several of the particle distributions usually presented in EAS calculations or measurements. We shall present some of the results for the 275 EAS calculated with the enhanced Fe abundance suggested by our results,^{18,19} and those of others²⁰ for $E_0 > 1000$ GeV. Our approach has been to attempt to simulate experiments by sampling both primary energy and mass in the calculated EAS. Thus, our results are perhaps better compared with EAS measurements rather than with other EAS calculations, which are usually done for a fixed primary energy and mass. For the latter comparison, however, our sampled energy spectrum yields a mean energy $E_0 \approx 2500$ GeV (median ≈ 1500 GeV), while the mean primary mass was $A \approx 22$.

In Fig. 1, the longitudinal development curves of the muon, pion, and nucleon mean numbers (per EAS) are plotted for core radii $r \leq 40$ and 300 m. The latter distributions look very much like those calculated by others²¹ for the nucleonic cascades in much larger EAS. It is interesting to note that the number of "core muons"^{5,10} (i.e., $r \leq 40$ m) penetrating to our ~ 752 -g cm⁻² observation level is typically still $> 65\%$ of the maximum, whereas

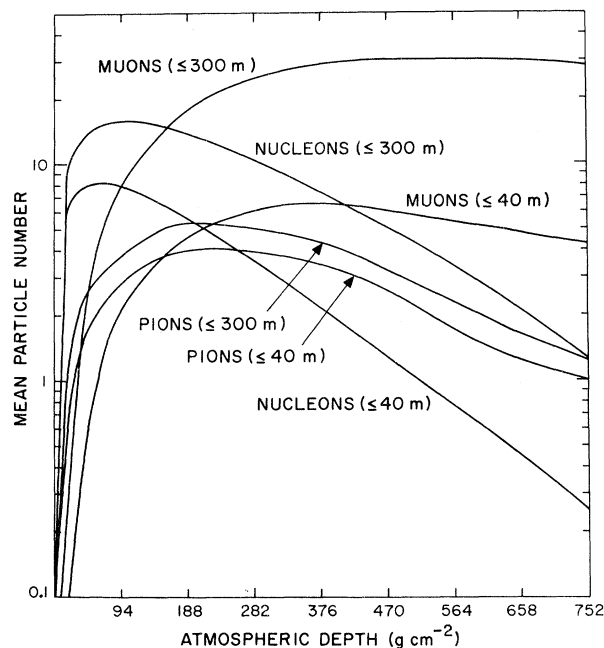


FIG. 1. Mean longitudinal distributions of 180 EAS. Sampled primary mass and $E_0 \geq 1 \times 10^{12}$ eV.

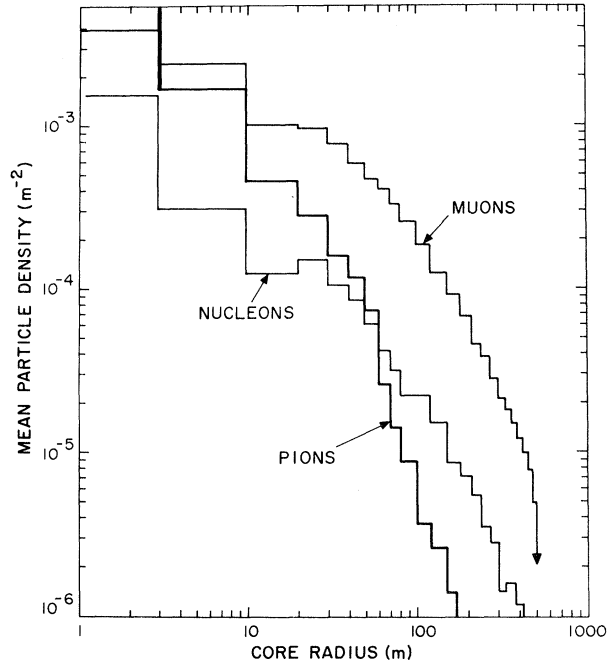


FIG. 2. Average lateral distributions from 180 EAS with $E_0 \geq 1 \times 10^{12}$ eV at 564 g cm⁻². Particles were not followed beyond $r > 500$ m (downward arrow).

the pion and nucleon components are attenuated much more rapidly.

The average particle lateral distributions sampled at a depth of 564 g cm⁻² are shown in Fig. 2. As before,¹⁰ particles were sampled at 564 g cm⁻² since that is the approximate depth from which their Čerenkov light production may be detected by spaced, mountain-altitude (~ 750 g cm⁻²) detectors (see below and Fig. 6). It is also about the minimum depth (i.e., Mt. Chacaltaya) for actual EAS particle-detection arrays. The pion distribution is much steeper than that for muons, as for large EAS,²¹ since pions will usually have decayed or interacted before traveling a great distance.

Since the lateral distributions are the most easily measurable for EAS large enough to be directly detected by particle-detection arrays, it is interesting to compare these results with extrapolations from other calculations and from direct measurements of much larger showers. Since the total muon number is the most nearly constant EAS parameter beyond the shower maximum (Fig. 1), we may compare our muon distributions (564 g cm⁻²) with those measured for much larger ($E_0 \sim 10^{15}$ – 10^{17} eV) EAS at sea level with minimal uncertainty due to differing shower age. It is rather remarkable that the expression found to match the observed muon density at $r = 500$ m, i.e.,

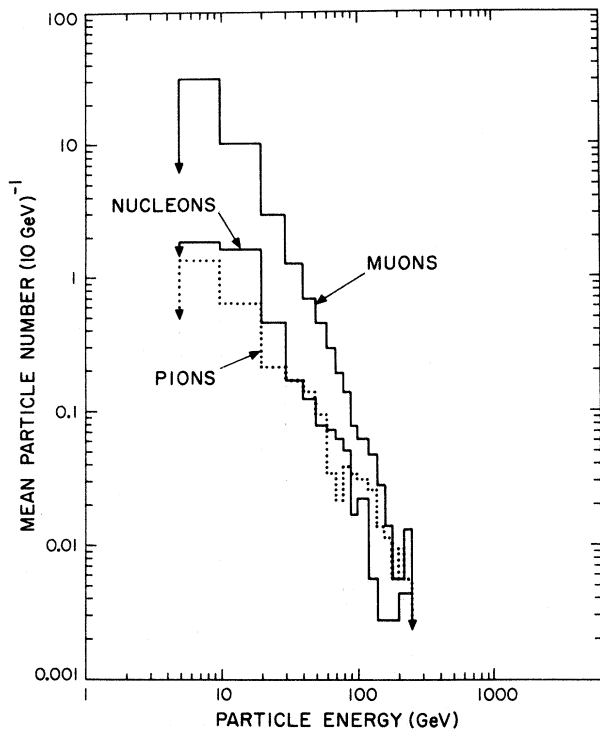


FIG. 3. Differential energy spectra of mean total-particle numbers at 564 g cm^{-2} from 180 EAS. Sampled primary mass and $E_0 \geq 1 \times 10^{12} \text{ eV}$; downward arrows mark the cutoffs in particle energies plotted.

$\rho_\mu(500) = 0.18(E_0/10^{17})^{0.92} \text{ m}^{-2}$, for the large EAS observed at Haverah Park,²² yields $\rho_\mu(500) = 9 \times 10^{-6} \text{ m}^{-2}$ for our mean energy of $E_0 = 2.5 \times 10^{12} \text{ eV}$. This is within a factor of 2 of our result in Fig. 2. The muon lateral density spectrum may be fitted by a power law $\rho_\mu \approx Kr^{-1.8}$ for $110 \leq r \leq 500 \text{ m}$; this is also consistent with the limiting index 1.82 found for Haverah Park data.²³ The agreement in these results may be fortuitous, although if the EAS are at similar ages, a smooth scaling of EAS (and, hence, interaction) observables with energy over some 5 decades in energy may be implied. This would suggest there are no very dramatic changes in the gross features of nuclear interactions over this largely unexplored energy range.

The differential energy spectra for the mean total muon, pion, and nucleon numbers present in the 180 calculated EAS sampled at 564 g cm^{-2} are given in Fig. 3. Again, we find in these results an interesting similarity with observations and calculations for much larger EAS. Our pion spectrum, for example, can be fitted well by a power law with exponent 1.60 from 10 to 200 GeV, or nearly the same slope indicated in a summary of results²² for EAS with $E_0 \sim 10^{15} \text{ eV}$. The muon

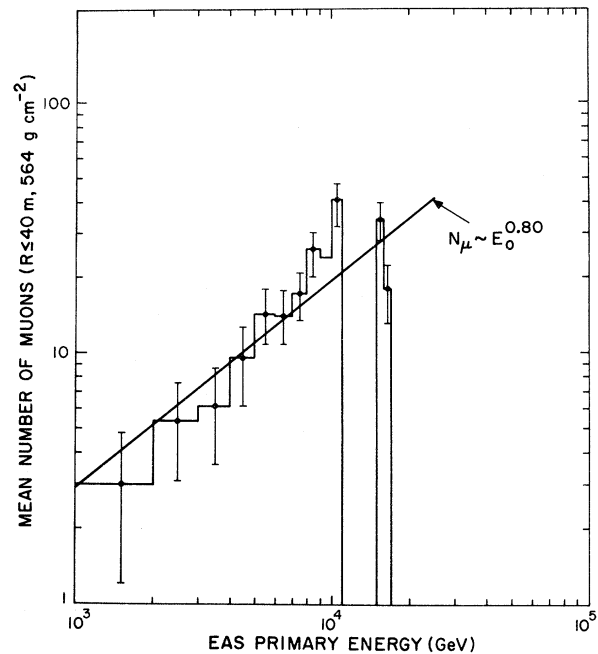


FIG. 4. Calculated distribution of average muon number within $r \leq 40 \text{ m}$ of axis at 564 g cm^{-2} from 208 EAS. Sampled primary mass and $E_0 \geq 1 \times 10^{12} \text{ eV}$.

differential spectrum is fitted well by a power law with index 2.48 in the same energy range. This compares very favorably with the integral spectrum index of 1.48 ± 0.19 measured for only an order of magnitude higher E_0 ($\sim 3 \times 10^{13} \text{ eV}$) at mountain altitudes.²⁴ The amplitude of the spectrum derived from these same measurements would give our value of ~ 33 muons ($E_\mu \geq 5 \text{ GeV}$) for a local shower size $N \sim 140$, or about the expected total at the depth sampled. Although we shall again postpone a discussion of the sensitivity of our results to the primary mass A , it is interesting to note that our early results¹⁰ for pure proton primaries gave significantly flatter muon energy spectra.

Finally, in Fig. 4, we give the calculated distribution at 564 g cm^{-2} of the mean (per EAS) muon number ($r \leq 40 \text{ m}$) as a function of primary energy. The power-law fit shown is $N_\mu \propto E_0^{0.8}$. This is the usual dependence obtained in the larger EAS results, since $N_e \propto E_0^{1.0}$.

We now turn to the results of the calculation of the Čerenkov photon yield at 2320-m elevation ($\sim 760 \text{ g cm}^{-2}$ depth) from the EAS Monte Carlo simulations. The calculation was done over the trajectory of each nuclear active particle (n.a.p.) and muon produced in 73 of the EAS stored on tape. The lateral distributions of optical (300–550 nm) photons are plotted in Fig. 5, where our results for the “muon component” (including n.a.p.)

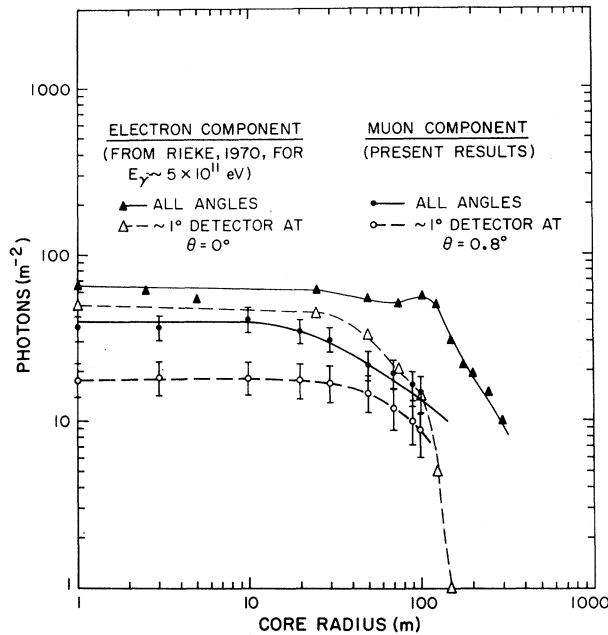


FIG. 5. Approximate Čerenkov photon lateral distributions: $E_{\text{cosmic ray}} \geq 1 \times 10^{12}$ eV, 2300-m elevation.

are compared with the results of Rieke⁸ for the electron component only. Our results, of course, refer to the sampled cosmic-ray primary mass and energy $E_0 \geq 1 \times 10^{12}$ eV. The electron-cascade Čerenkov component is for a total electromagnetic component energy of $\sim 5 \times 10^{11}$ eV and was obtained by simply scaling Rieke's results for 1×10^{11} eV γ -ray-initiated EAS. This choice of energy was dictated by the fact that in our results a total energy $\sim \frac{1}{3} E_0$ is lost to the π_0 component and, hence, to the electromagnetic cascade, for which we use Rieke's results, and that our median primary energy is 1.5×10^{12} eV. Zatsepin and Chudakov⁷ have compared the electromagnetic (em) component and resultant Čerenkov production in γ -ray vs cosmic-ray-initiated EAS and found similar lateral and angular photon distributions. The fact that most of the Čerenkov light detectable from the electrons comes from the EAS maximum makes the em components of the two shower types appear very similar¹⁰ and justifies the use of Rieke's results here. In Fig. 5 we have plotted distributions for the densities of all optical photons incident at a given core radius as well as the photon densities detectable by a 1° opening-angle detector, as is commonly used. For these latter distributions, the detector was "pointed" parallel to the EAS axis ($\theta = 0^\circ$) for the electron component and at zenith angle $\theta = 0.8^\circ$ toward the EAS axis for the muon component. It is interesting that then the muon and electron Čerenkov yields are comparable at core distances $r \approx 130$ m.

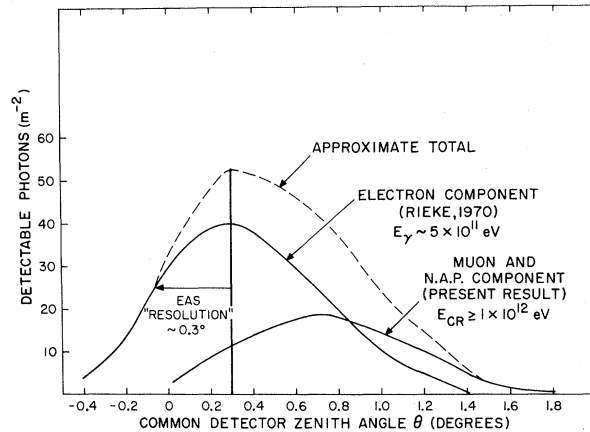


FIG. 6. Calculated Čerenkov angular distributions at $r \approx 40$ m from EAS axis at 2300 m as detected by $\sim 1^\circ$ light receivers.

In a sense, the primary objective of these calculations has been realized in Fig. 6, where we show the angular distributions of the calculated Čerenkov flux at a particular core radius ($r = 40$ m). This is the distribution most easily measured, and finding its two-component structure⁵ prompted our original investigation.¹⁰ Figure 6 shows our results for the muon and n.a.p. components and those of Rieke⁸ for the electron component, as each would be detected by 1° light receivers. The detector is assumed to be pointing in azimuth at the EAS axis and in elevation at angle $90^\circ - \theta$ toward the axis (negative θ values indicate the azimuth angle points 180° away from the axis). The combined total is also shown. No atmospheric absorption or detector spectral response factors are included. For comparison with observation,⁵ it is vital to include the exact spectral response of the detector, since atmospheric UV (ultraviolet) attenuation will be much less for the muon component with path lengths ~ 2 km (typically) than for the electron component (~ 7 km). Then, because the Čerenkov production spectrum varies as λ^{-2} , the muon component of the angular distribution can be comparable to the electron component if the detectors are biased toward the UV (e.g., 280–400 nm). We also found that for differing detection-core radii, the muon component peak in the angular distribution remains at $\theta \sim 0.8^\circ$ (\sim the observed⁵ UV peak), since it is approximately the Čerenkov opening angle that is detected rather than a unique height of maximum muon number. Indeed, Fig. 1 shows that the muon number declines only very slowly with depth. The electron component angular maximum, however, is linearly dependent on core radius since it is simply the greatly enhanced electron number at EAS maximum that is detected.

Finally, we repeated our Čerenkov calculations for a random sampling of shower impact radii and arrival directions within the $\sim 0.3^\circ$ (half-angle) EAS resolution cone of a spaced detector pair pointed at the electron maximum. The muon Čerenkov angular distribution was again found to be very similar to that in Fig. 6.

IV. CONCLUSIONS

We have carried out Monte Carlo simulations of EAS nuclear cascades incorporating recently observed multiplicities and cross sections for the interactions as well as a full three-dimensional treatment. We attempted to simulate actually observed showers by random sampling of both primary mass (including observed fragmentation probabilities) and primary energy E_0 . The calculations have yielded particle spectra in surprisingly close agreement with extrapolations over several decades of E_0 from analytic fits to data (as a function of E_0) obtained for very large EAS. We have calculated the explicit contribution of the nuclear cascade and muon component to the at-

mospheric Čerenkov photon content of these EAS with $E_0 \geq 1 \times 10^{12}$ eV and found good agreement with our earlier observations. This demonstrates that the muon component is detectable in these small EAS solely by Čerenkov techniques. It is then possible to search selectively for γ -ray- (or electron-) initiated EAS as muon-poor events, and, indeed, this has formed the basis of our efforts¹⁰ to detect cosmic γ -ray sources at $E_\gamma > 10^{11}$ eV. The separate Čerenkov detection of EAS muon and electron components has also permitted preliminary studies of cosmic-ray composition.^{18,19} A complete analysis of these composition data will be presented separately, using the EAS calculations detailed here and, especially, their dependences on the cosmic-ray primary mass A .

ACKNOWLEDGMENTS

We thank the Smithsonian Astrophysical Observatory for providing generous computer time for this work, Dr. C. J. Waddington for kindly providing fragmentation probabilities, and the Society of Fellows of Harvard University for support.

- ¹W. Galbraith and J. V. Jelley, *Nature* **171**, 4347 (1953).
²F. I. Boley, *Rev. Mod. Phys.* **36**, 792 (1964).
³N. M. Nesterova, *Can. J. Phys.* **46**, S92 (1968).
⁴A. S. Krieger and H. V. Bradt, *Can. J. Phys.* **46**, S87 (1968).
⁵J. E. Grindlay, *Nuovo Cimento* **2B**, 119 (1971).
⁶C. Castagnoli, P. Picchi, and M. A. Locci, *Nuovo Cimento* **9B**, 213 (1972).
⁷V. I. Zatsepin and A. E. Chudakov, *Zh. Eksp. Teor. Fiz.* **42**, 1622 (1962) [*Sov. Phys.—JETP* **15**, 1126 (1962)].
⁸G. H. Rieke, Smithsonian Astrophysical Observatory Special Report No. 301, 1970 (unpublished).
⁹G. Bosia, M. Maringelli, and G. Navarra, *Nuovo Cimento* **9B**, 177 (1972).
¹⁰J. E. Grindlay, Smithsonian Astrophysical Observatory Special Report No. 334, 1971 (unpublished).
¹¹C. F. Powell, P. H. Fowler, and D. H. Perkins, *Study of Elementary Particles by the Photographic Method* (Pergamon, London, 1959).
¹²C. J. Waddington, private communication (1973).
¹³G. B. Yodh, Yash Pal, and J. S. Trefil, *Phys. Rev. Lett.* **28**, 1005 (1972).
¹⁴F. T. Dao, D. Gordon, J. Lach, E. Malamud, T. Meyer, R. Poster, and W. Slater, *Phys. Rev. Lett.* **29**, 1627 (1972).
¹⁵E. L. Berger, *Phys. Rev. Lett.* **29**, 887 (1972).
¹⁶V. L. Ginzburg and S. I. Syrovatskii, *Origin of Cosmic*

Rays (MacMillan, New York, 1964).

- ¹⁷J. V. Jelley, *Čerenkov Radiation and Its Applications* (Pergamon, London, 1958).
¹⁸J. E. Grindlay, in *Proceedings of the Twelfth International Conference on Cosmic Rays, Hobart, 1971*, edited by A. G. Fenton and K. B. Fenton (Univ. of Tasmania Press, Hobart, Tasmania, 1971), Vol. 7, p. 2730.
¹⁹J. E. Grindlay and H. F. Helmken, in *Proceedings of the Thirteenth International Conference on Cosmic Rays, Denver, 1973* (Colorado Associated Univ. Press, Boulder, 1973), Vol. 1, p. 202.
²⁰J. F. Ormes and V. K. Balasubrahmanyam, *Nature Phys. Sci.* **241**, 95 (1973).
²¹K. E. Turver, Univ. of Durham, England, report, 1973 (unpublished).
²²H. E. Dixon, J. C. Earnshaw, J. R. Hook, G. J. Smith, and K. E. Turver, in *Proceedings of the Thirteenth International Conference on Cosmic Rays, Denver, 1973* (Ref. 19), Vol. 4, p. 2473.
²³P. R. Blake, H. Ferguson, and W. F. Nash, in *Proceedings of the Twelfth International Conference on Cosmic Rays, Hobart, 1971*, edited by A. G. Fenton and K. B. Fenton (Ref. 18), Vol. 3, p. 1056.
²⁴A. D. Erlykin, in *Proceedings of the Thirteenth International Conference on Cosmic Rays, Denver, 1973* (Ref. 19), Vol. 4, p. 2500.